Data
Models
Inventories

PARIS

Process Attribution of Regional Emissions

GA 101081430, RIA

Complete calendar year of extended and quality controlled N2O data uploaded to the ICOS portal, included in D5.2

M41			
Delivery due date Annex I	01/05/2025		
Actual date of submission	01/02/2026		
Lead beneficiary: EMPA	Work package: 5	Nature: Report/data	Dissemination level: Public
Responsible scientist	Stephan Henne		
Contributors	Haszpra László ATOMKI, Anita Ganesan UNIVBRIS, Alistair Manning MO		
Internal reviewers			
Version: xx			

Horizon Europe Cluster 5: Climate, energy and mobility

"This project has received funding from the European Union's Horizon Europe Research and Innovation programme under HORIZON-CL5-2022-D1-02 Grant Agreement No 101081430 - PARIS".

Table of content

1. Changes with respect to the DoA (Description of the Action)

While the report was delivered with delay, the relevant data were uploaded to the ICOS Carbon Portal on time for use in the associated inverse modelling tasks.

2. Dissemination and uptake

The data collected/produced as part of this milestone are relevant for the production of the Annex reports in WP2. As such they have been shared with the relevant project partners prior to the completion of D5.2 and D2.3. Final data products are all available publicly on the ICOS Carbon Portal for use by other scientists and practitioners.

3. Short Summary of results

Atmospheric observations of N_2O mole fractions from the site directly supported by the PARIS project, Hegyhátsál (Hungary), and other non-ICOS sites (UK and Swiss sites) for the period up to April 2025 were submitted to the ICOS ATC collection of European N_2O (ObsPack Europe, https://doi.org/10.18160/T18D-C85R). The submission required critical quality control of the acquired observations, calibration on WMO scales and harmonisation of data formats and metadata.

The near-complete ObsPack was then used as input to the inversion modelling systems employed in PARIS, combining a total of six combinations of inversion system (RHIME, InTEM, ELRIS) and transport models (NAME, FLEXPART). Inverse modelling results include monthly N_2O fluxes at a spatial resolution of 25 km x 25 km and country aggregates for the European domain. These were collected in commonly defined data formats and made publicly available (https://doi.org/10.18160/GR1Q-6SK4).

4. Evidence of accomplishment

Individual time series of atmospheric observations of N_2O funded by PARIS are available on the ICOS Carbon Portal:

HUN, Hungary, https://meta.icos-cp.eu/objects/HNQFgSCrfNCRYrul3HNikPUU, PARIS funding

Non-ICOS atmospheric observations of N_2O by PARIS partners are available on the ICOS Carbon Portal:

BRM, Switzerland, https://meta.icos-cp.eu/objects/-Baxb0WyxFtY-fD6b4e1V2qC, EMPA

TAC, UK, https://meta.icos-cp.eu/objects/4iL4GGVScAtVew6wdyhaxhob, UNIVBRIS

HFD, UK, https://meta.icos-cp.eu/objects/l-e47vwBi7x2PFy2RgcRMmBf, UNIVBRIS

MHD, IRL, https://meta.icos-cp.eu/objects/6sBlpGeQNvSpnmwU03YIuMsD, UNIVBRIS

Inverse modelling results (including flux estimates as well as observed and simulated atmospheric mole fractions) from the individual inversions are available on the ICOS Carbon Portal:

ELRIS-FLEXPART, https://meta.icos-cp.eu/objects/FTUWRIr4Un4fETBUgcQp4qHA

ELRIS-NAME, https://meta.icos-cp.eu/objects/MOJbmoZ-f42MBphbpFY3bGDb

InTEM-FLEXPART, https://meta.icos-cp.eu/objects/ZILjPVFmFANnim9bpe9UCqAe
InTEM-NAME, https://meta.icos-cp.eu/objects/TlAicGVTtNRABBoycqSgrQzO
RHIME-FLEXPART, https://meta.icos-cp.eu/objects/WryaayEmhxy6Um7jsc_ZyQQQ
RHIME-NAME, https://meta.icos-cp.eu/objects/Sct_2uBOLpeJB4gHRSultN1r

4.1 Introduction | Background of the milestone

Observations of greenhouse gases form the backbone of any inverse estimate of greenhouse gas fluxes to the atmosphere. The landscape of atmospheric N_2O observations in Europe was traditionally driven by individual research groups deploying instrumentation at a small number of sites within the continent. In addition, NOAA's flask sampling program included various European sites, both on the continent and remote baseline sites over the ocean. With the advent of ICOS new N_2O observations became available through the ICOS Carbon Portal after 2017 following the strict ICOS data quality requirements. In contrast to traditional GC-ECD observations, ICOS requires laser spectroscopy instrumentation, achieving much better precision and measurement frequency. Similarly, several non-ICOS sites were equipped with laser-based instrumentation after 2017, but data were not collected in a uniform format. After the initial effort of collecting N_2O observations in the PARIS, EYECLIMA and AVENGERS projects (see D5.1), the ICOS ATC has taken up the task of annually collecting non-ICOS observations of the major greenhouse gases (CO_2, CH_4, N_2O) as part of their European ObsPacks. PARIS directly supports the N_2O observations at the tall tower Hegyhátsál, Hungary, whereas other non-ICOS N_2O observations of PARIS partners are provided as in-kind contributions to the European ObsPack. Previously, N_2O observations at the tall tower site Hegyhátsál, Hungary were carried out for assessing the local N_2O flux (eddy covariance method). Since the eddy covariance method does not necessarily require absolute calibration of the analyser, a complete calibration setup had not been installed at the site. As part of PARIS, a calibration strategy for the Hegyhátsál N_2O analyser was devised, largely following ICOS recommendations (see PARIS milestone M17 for details on instrumentation and calibration). A quality control procedure was established, and observations automatically and manually checked for invalid observations. Here an update of the observations until March 2025 is discussed.

Inverse estimates of N_2O are made using the mentioned atmospheric measurements of mole fractions. Use of atmospheric transport models is necessary to translate these atmospheric measurements into estimates of emissions from the surface. Multiple methods and analyses can be used to couple models with atmospheric data, which can vary significantly, for example through the data filtering methodologies, resolution of the transport model output, transport model setup, and execution of the statistical inversion technique. Team members have each published their own independent methods and results on the use of their inversion systems in estimating greenhouse gas emissions (e.g., Manning et al., 2021; Redington et al., 2023; Katharopoulos et al., 2023; Henne et al., 2016; Ganesan et al., 2015). A detailed common description of the inversion systems and their specific setup for PARIS was compiled as an annex to PARIS deliverable D2.3.

Throughout the project, N_2O emissions estimates are derived for Europe across a matrix of transport models and inversion setups, using new observations collected in the project (University of Bristol: RHIME-NAME, RHIME-FLEXPART; Met Office: InTEM-NAME InTEM-FLEXPART; EMPA: ELRIS-NAME and ELRIS-FLEXPART).

4.2 Scope of the milestone

This milestone forms the basis for the inverse modelling results that form deliverable D5.2 and are in turn used in the draft Annexes provided to the national inventory teams for their 2026 reporting to the UNFCCC (D2.3).

4.3 Content of the milestone

4.3.1 Overview

This report covers two parts: 1) a brief description of the observational data contributed by PARIS to the European ObsPack and an overview of data availability for inverse modelling, 2) a description of the applied inversion systems and their performance evaluation against observations. The results of the inversions (monthly N_2O fluxes for the period 2016 to 2024) are discussed in deliverable D5.2.

4.3.2 Observations and network sensitivity

Atmospheric N_2O mole fraction observations continued at the tall tower at Hegyhátsál, Hungary, using an inlet height 82 m above ground. Fig. 1 compares hourly aggregates of these observations to the closest ICOS sites (Hohenpeissenberg, HPB, Germany) and (Křešín u Pacova, KRE, Czech Republic) for the years 2022 to 2024. In general, parallel evolution of the background mole fractions (for now we consider these to be reflected by the lower envelope of the data) and trends can be discerned. Observed peak sizes were largest for HUN and were largest in late spring, early summer, indicating intense seasonality in N_2O emissions in the region around the site. The similarities in the background mole fractions suggest that no major calibration issues persist between these sites. However, differences in the range below 0.5 ppb are difficult to detect from this comparison. Fig. 2 gives an overview of all N_2O observations available for and used by the different inversion systems. Note that some sites did not yet provide data for 2024 or stopped monitoring N_2O earlier on. A total of 29 sites are listed in the figure, and all the displayed data were used in the inversions. Next to mole fraction, the observational data also contains estimates of measurement uncertainty (understood as the repeatability of a mole fraction observation, estimated from target gas measurements) and the sub-hourly variability of the observations. The latter is used by the inversion systems as a proxy for model uncertainty as situations with large observed mole fraction variability are considered to align with situations in which the models have difficulties reflecting these variabilities and, consequently, also the mean.

The combined 'coverage' of the N_2O observations is depicted in Fig. 3 as the simulated (transport model FLEXPART) average source sensitivity for the year 2018 and 2024. The start of many ICOS sites since 2018 has largely improved the spatial coverage of the European N_2O observational network.

Especially well covered north-western European countries including the UK, France, the Benelux area, Germany, Czech Republic, Switzerland and northern Italy.

The PARIS funded observations in Hungary significantly improve the network's ability to see emissions from Hungary but also from Austria. Beyond these regions, the measurement network remains poor and inverse emission estimates for countries outside the regions described will remain of limited quality.

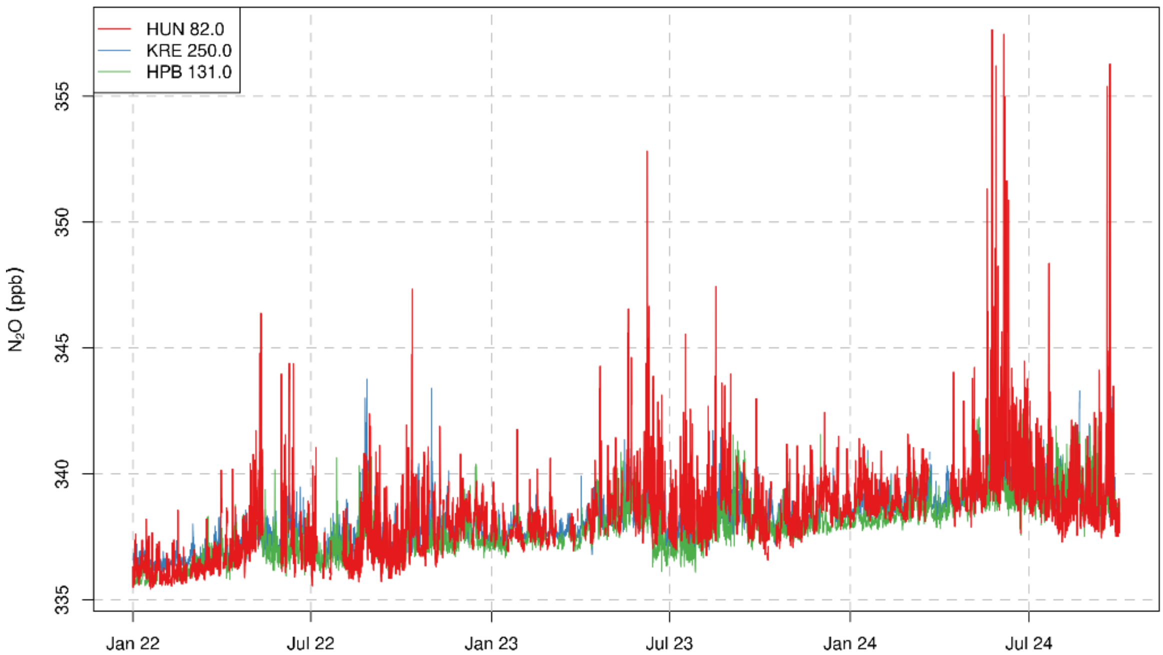

Fig. 1: Time series of fully calibrated N_2O observations (1-hour averages) from Hegyhátsál (red) compared to those carried out at closest ICOS sites HPB, Germany, (green) and KRE, Czech Republic, (blue). Note that only data from 2022 to the end of the common data period is shown (end of Aug 2024 for ICOS sites at time of comparison).

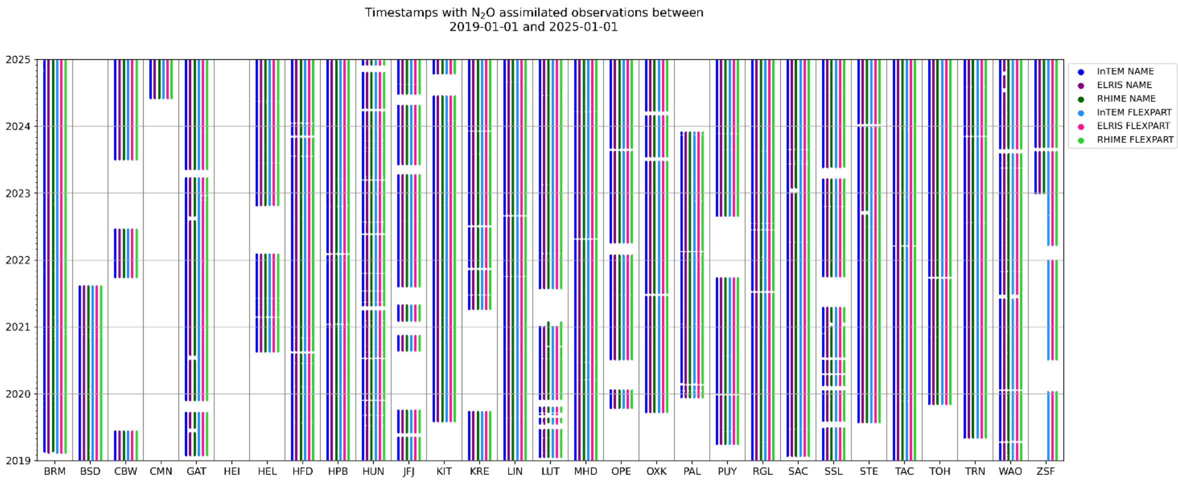

Fig 2: N_2O observational data usage by the different employed inversion models for the period 2019 to 2024. Note that some sites did not report any data during this period (but previously), whereas other sites stopped reporting.

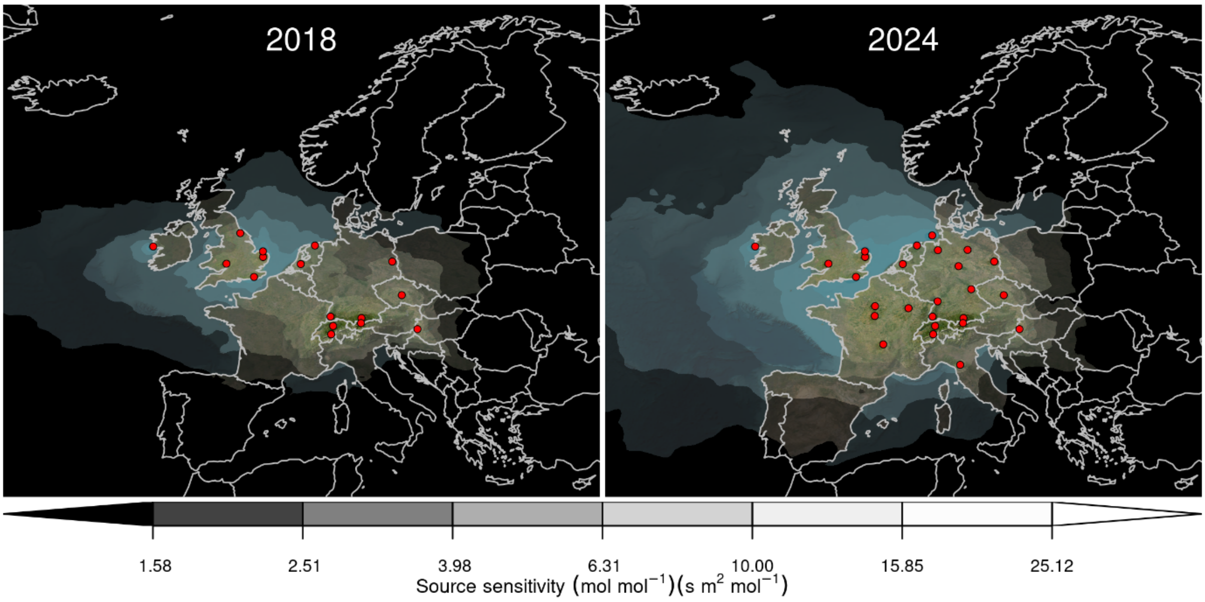

Fig. 3: Average monthly total source sensitivity of N2O observing sites as calculated by the FLEXPART transport model for the year 2018 (left) and 2024 (right) and used in the inversions. Observing stations active in each year are marked with red dots. Areas with visible land surface represent regions for which emissions can be observed well from the network. Shaded or dark areas represent regions for which limited emission information can be obtained from the network.

4.3.3 Inversion setup

A detailed description of the inverse model setup for the PARIS N_2O inversions is provided as part of deliverable D2.3 and serves as documentation for the inventory teams. It includes both a comprehensive discussion of the employed inversion techniques as well as the specific settings used for the N_2O inversions.

In short, all three inversion systems (RHIME, InTEM, ELRIS) can be run with source sensitivities calculated by the atmospheric transport models FLEXPART or NAME. A common data format for the source sensitivities allows flexible exchange of one transport with the other. All three inversion systems have in common that the state vector, which is optimised as part of the inversion, contains emission and baseline elements. In all systems, a spatial aggregation of the emissions to larger areas (basis functions) is undertaken, but the details differ in terms of structure and number of state vector elements between the different systems. The baseline is treated by estimating the mole fractions at eleven interfaces around the common transport domain. The sensitivity of an observation to a baseline interface differs with time and is determined by the transport models as well. Common prior emissions are employed in all three models based on EDGAR 8.0 N_2O emissions. However, each modelling group made their own choices in terms of prior uncertainty and covariance structure. Mostly the same observations were used by all inversion systems (compare Fig), but somewhat different filtering strategies, to avoid times with large model uncertainty, were employed. Different strategies were employed to determine the so-called model data mismatch uncertainty. Commonly, different sources of uncertainty (instrumental, model, baseline) were considered, but details differ between the systems.

4.3.4 Inversion performance analysis

An example N_2O time series as observed and simulated at the site Hegyhátsál (HUN), Hungary, is given in Fig. 4. For each model system the figure shows the observations, the prior simulated mole fractions and the simulated mole fractions after emission optimisation (posterior simulation). Although the prior simulated time series already follows the observed time series well, the match is improved through the optimisation process as can also be seen in a reduced bias and RMSE as indicated in the histograms on the right. As seen above, the site is characterised by sharp pollution peaks in the summer months. These are only partly picked up by the simulations, which could indicate larger local to regional sources than estimated in the posterior.

Similarly, performance parameters were calculated for all sites and all model systems (Fig. 5). In many cases, posterior Pearson correlation coefficients were larger than 0.8, with only very few exceptions with correlation coefficients smaller than 0.6 being observed. No systematic difference in terms of performance can be discerned for different inversion systems and utilised transport models. The mean posterior bias was below 0.1 ppb in most cases. Centered RMSE were largely below 0.5 ppb, exceptions being LUT in the Netherlands and HUN in Hungary (both sites are situated in areas with large agricultural N_2O fluxes).

The Taylor plots in Fig. 6 serve as additional proof of how comparison statistics were improved through the inversion. In this plot, posterior values generally are located closer to the expectation of a perfect model (correlation coefficient and normalized standard deviation of one) than their prior companions. Improvements for individual sites differ from model to model, but the general trend is the same for all inversions.

Although time series performance statistics are not an unambiguous proof that the obtained inversion results are close to the unknown true state, they still serve as an important indicator for an accurate setup and successful application of the inversion systems.

Fig. 4: Observed (black dots) and simulated (lighter colors prior, darker colors posterior) N2O mole fractions at the site Hegyhátsál (HUN) at the Irish west coast. Each sub-panel represents the comparison to one of the six inversion runs. The error bars give the model data mismatch uncertainty assumed by each model. The histograms on the right give the prior (lighter) and posterior (darker) model-observation residuals, with μ and σ representing the mean bias an RMSE, respectively.

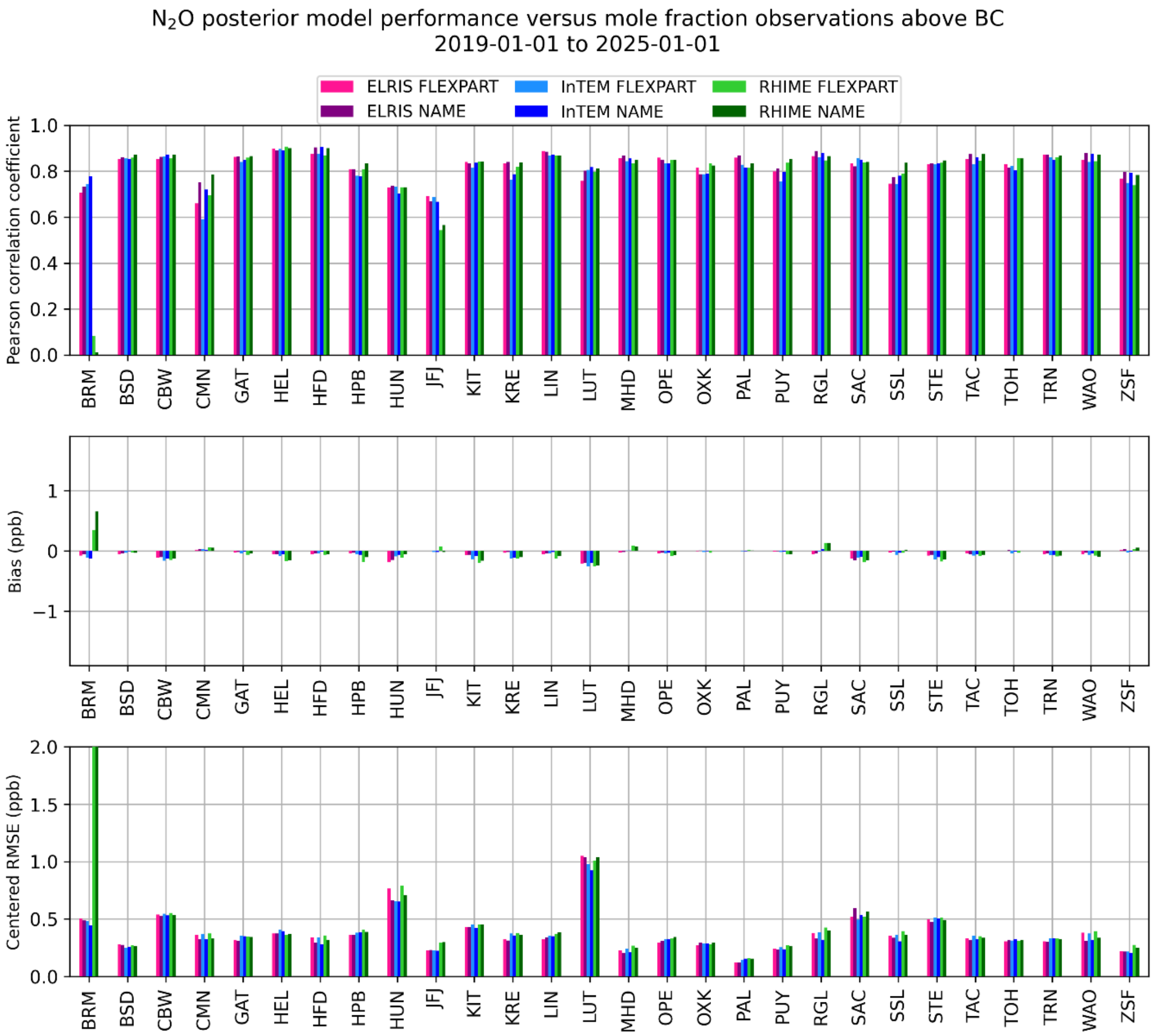

Fig. 5: Posterior model performance characterised by Pearson correlation coefficients (top), mean bias (middle), and centered RMSE (bottom) between observed simulated mole fractions above the baseline for all sites assimilated in the inversion and all model systems. Performance parameters were calculated for all observations in the period 2019 to 2024.

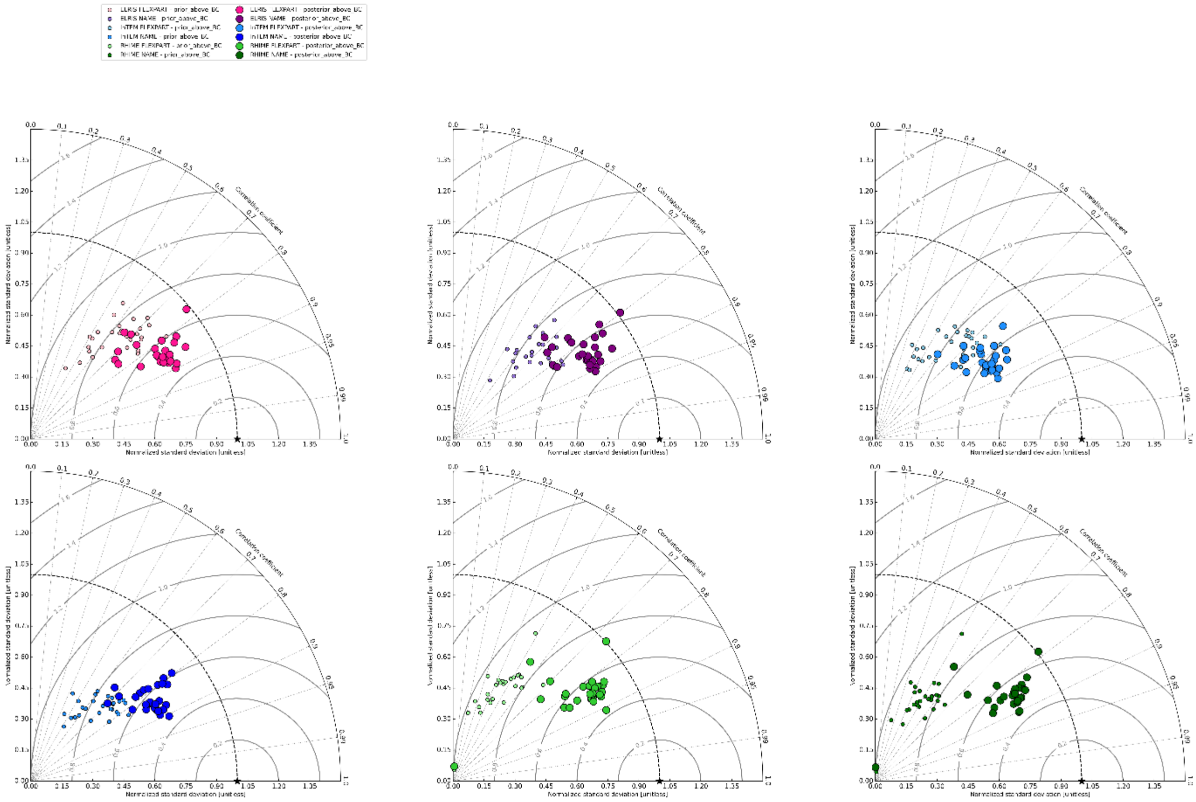

Fig. 6: Taylor plot of prior (small dots) and posterior (large dots) simulated posterior above-baseline mole fractions for the period 2019 to 2024 and separate for each model system.

4.4 Conclusion and possible impact

The collection of high-frequency N_2O observations from European sites and the set up and successful application of six inverse modelling systems allows for a robust estimation of N_2O fluxes in north-western Europe. Fluxes will be reported as part of PARIS deliverable D5.2 and conclusions on the country level are reported to the respective national inventory teams as part of PARIS deliverable D2.3.

4.5 References

Ganesan, A. L., Manning, A. J., Grant, A., Young, D., Oram, D. E., Sturges, W. T., Moncrieff, J. B., and O'Doherty, S.: Quantifying methane and nitrous oxide emissions from the UK and Ireland using a national-scale monitoring network, Atmos. Chem. Phys., 15, 6393-6406, doi: 10.5194/acp-15-6393-2015, 2015.

Henne, S., Brunner, D., Oney, B., Leuenberger, M., Eugster, W., Bamberger, I., Meinhardt, F., Steinbacher, M., and Emmenegger, L.: Validation of the Swiss methane emission inventory by atmospheric observations and inverse modelling, Atmos. Chem. Phys., 16, 3683-3710, doi: 10.5194/acp-16-3683-2016, 2016.

Katharopoulos, I., Rust, D., Vollmer, M. K., Brunner, D., Reimann, S., O'Doherty, S. J., Young, D., Stanley, K. M., Schuck, T., Arduini, J., Emmenegger, L., and Henne, S.: Impact of transport model resolution and a priori assumptions on inverse modeling of Swiss F-gas emissions, Atmos. Chem. Phys., 23, 14159–14186, doi: 10.5194/acp-23-14159-2023, 2023.

Manning, A. J., Redington, A. L., Say, D., O'Doherty, S., Young, D., Simmonds, P. G., Vollmer, M. K., Mühle, J., Arduini, J., Spain, G., Wisher, A., Maione, M., Schuck, T. J., Stanley, K., Reimann, S., Engel, A., Krummel, P. B., Fraser, P. J., Harth, C. M., Salameh, P. K., Weiss, R. F., Gluckman, R., Brown, P. N., Watterson, J. D., and Arnold, T.: Evidence of a recent decline in UK emissions of hydrofluorocarbons determined by the InTEM inverse model and atmospheric measurements, Atmos. Chem. Phys., 21, 12739–12755, doi: 10.5194/acp-21-12739-2021, 2021.

Redington, A. L., Manning, A. J., Henne, S., Graziosi, F., Western, L. M., Arduini, J., Ganesan, A. L., Harth, C. M., Maione, M., Mühle, J., O'Doherty, S., Pitt, J., Reimann, S., Rigby, M., Salameh, P. K., Simmonds, P. G., Spain, T. G., Stanley, K., Vollmer, M. K., Weiss, R. F., and Young, D.: Western European emission estimates of CFC-11, CFC-12 and CCl4 derived from atmospheric measurements from 2008 to 2021, Atmos. Chem. Phys., 23, 7383–7398, doi: 10.5194/acp-23-7383-2023, 2023.

5. History of the document

Version	Author(s)	Date	Changes
1.0	Stephan Henne	2025-09-01	Frist draft